Solution X-ray Scattering Data Show Structural Differences among Chimeras of Yeast and Chicken Calmodulin: Implications for Structure and Function†

Tsuyoshi Yokouchi,‡ Hideki Nogami,‡ Yoshinobu Izumi,*,‡ Hidenori Yoshino,§ Ken-ichi Nakashima,|| and Michio Yazawa||

Graduate Program of Human Sensing and Functional Sensor Engineering, Graduate School of Science and Engineering, Yamagata University, Yonezawa 992-8510, Japan, Department of Chemistry, Sapporo Medical University, Sapporo 060-0061, Japan, and Division of Chemistry, Graduate School of Science, Hokkaido University, Sapporo 060-0810, Japan

Received July 31, 2002; Revised Manuscript Received November 26, 2002

ABSTRACT: We present here the first evidence, obtained by the use of small-angle X-ray scattering, of the solution structures of chimeras constructed from yeast (*Saccharomyces cerevisiae*, Sc) and chicken (*Gallus gallus*, Gg) calmodulin (CaM). The chimeric proteins used in this study are $Sc^{1-129}/Gg^{130-148}$, $Sc^{1-128}/Gg^{129-148}$, Sc^{1-87}/Gg^{88-148}, and Sc^{1-72}/Gg^{73-148} CaMs, in which Sc^{1-n} and $Gg^{(n+1)-148}$ descend from yeast and chicken CaM in the chimeric proteins, respectively. Under the Ca^{2+}-saturated condition, the solution structure of $Sc^{1-128}/Gg^{129-148}$ CaM has a dumbbell-like shape which is characteristic of vertebrate-type CaM, while that of $Sc^{1-129}/Gg^{130-148}$ CaM takes an intermediate structure between the dumbbell-like shape and a compact globular shape. The results provide the direct evidence that the replacement of Asp^{129} with Ser^{129} induces an interaction between two lobes of $Sc^{1-129}/Gg^{130-148}$ CaM and brings them close together. It implies that a site interacting with the N-lobe is induced in the C-lobe, although site IV that is unable to bind Ca^{2+} hinders the ability of the C-lobe to undergo the conformational change to the full open state. In the presence of both Ca^{2+} and a peptide synthesized to mimic the CaM binding domain on myosin light chain kinase, MLCK-22p, the solution structures of these chimeric CaMs take a similar compact globular shape but their interactions are quite different. The solution structure and interactions of Sc^{1-72}/Gg^{73-148} CaM are similar to those of Sc^{1-87}/Gg^{88-148} CaM. The structure of Sc^{1-87}/Gg^{88-148} CaM is similar to that of $Sc^{1-128}/Gg^{129-148}$ CaM, but their interactions are different. The result indicates that the replacement of Glu^{119} with Ala^{119} has a critical effect on their interactions. Thus, the functional differences among these chimeric CaMs, which have been reported previously [Nakashima, K., et al. (1996) *Biochemistry 35*, 5602−5610], have been interpreted on the basis of the structures and interactions.

Calmodulin (CaM)[1] is small protein which appears in all eukaryotic cells and regulates many significant cellular functions as a versatile decoder of Ca^{2+} signals. The crystal structure of Ca^{2+}-saturated vertebrate CaM resembles a dumbbell in which the N-lobe is connected to the C-lobe by a central linker helix of approximately eight turns (*1*−*3*). A pair of Ca^{2+}-binding sites is located in each of the lobes (Ca^{2+}-binding sites I and II in the N-lobe and sites III and IV in the C-lobe). The Ca^{2+} binding affinity of the C-lobe is higher than that of the N-lobe (*4*). Much effort has been devoted to revealing the structure−function relationships of CaM. The major questions are the functional significance of the dumbbell shape and the functional differences among the four Ca^{2+}-binding sites.

The primary structure of CaMs is extremely conservative, and the homology of the sequence is greater than 90% among vertebrates and invertebrates (*5*). The primary structure of CaM from baker's yeast (*Saccharomyces cerevisiae*, Sc; yeast CaM), however, is only 60% identical with that of vertebrate CaM (*6*). Functionally, yeast CaM does not bind Ca^{2+} at site IV; the set of macroscopic association constants of yeast CaM is also different from others (*7*, *8*), and yeast CaM is a poor activator of vertebrate enzymes (*9*, *10*). Recent results of solution X-ray scattering, NMR, and biochemical studies suggest an unusual mode of target recognition, which is different from the typical one of vertebrate CaM (*11*−*15*).

To elucidate aspects of the structure−function relationship of yeast CaM, we have used four kinds of chimeric proteins of chicken (*Gallus gallus*, Gg) and yeast CaM in which the

† This work was supported in part by a Grant-in-Aid for Scientific Research from the Ministry of Education, Science, and Culture, Japan (Proposal 10450358 to Y.I.). SAXS measurements were performed with the approval of the Photon Factory Advisory Committee, KEK, Tsukuba, Japan (Proposals 95G274 and 97G131).

* To whom correspondence should be addressed: Graduate Program of Human Sensing and Functional Sensor Engineering, Graduate School of Science and Engineering, Yamagata University, Yonezawa 992-8510, Japan. Fax: 81-238-26-3177. E-mail: yizumi@yz.yamagata-u.ac.jp.

‡ Yamagata University.

§ Sapporo Medical University.

|| Hokkaido University.

[1] Abbreviations: CaM, calmodulin; PDE, cyclic nucleotide phosphodiesterase; skMLCK, skeletal muscle myosin light chain kinase; NMR, nuclear magnetic resonance; K_{act}, concentration of CaM required for half-maximal activation; V_{max}, maximum activity; SR-SAXS, small-angle X-ray scattering using synchrotron radiation; R_g, radius of gyration at a finite concentration; R_0, radius of gyration at infinite dilution; B_{if}, parameter of interparticle interference; A_2, second virial coefficient; $P(r)$, distance distribution function; d_{max}, maximum distance of the particle; R_{lobe}, radius of gyration of the lobe; L, center-to-center distance between two lobes.

10.1021/bi020501s CCC: $25.00
Published on Web 01/30/2003

Table 1: Functional Properties of CaMs[a]

		PDE		skMLCK	
	Ca^{2+} binding numbers	V_{max} (%)	K_{act} (nM)	V_{max} (%)	K_{act} (nM)
Gg^{1-148}	4	103	1.14	103	2.4
Sc^{1-72}/Gg^{73-148}	4	97.2	1.74	84.2	48.6
Sc^{1-87}/Gg^{88-148}	4	104	2.71	87.0	70.0
$Sc^{1-128}/Gg^{129-148}$	4	102	5.45	53.7	3440
$Sc^{1-129}/Gg^{130-148}$	3	96.3	52.0	14.7	8070
Sc^{1-146}		95.5	4310	9.9	41300

[a] The data are taken from a previous report (*16*).

N-terminal sequences of chicken CaM were substituted for the corresponding regions of yeast CaM. Table 1 summarizes previous results on the activation profiles of phosphodiesterase (PDE) and skeletal myosin light chain kinase (skMLCK) by these proteins (*16*). Here, Gg^{1-148} and Sc^{1-146} denote chicken CaM and yeast CaM, respectively, and the chimera of $Sc^{1-n}/Gg^{(n+1)-148}$ consists of residues in the yeast CaM sequence of $1-n$ and chicken CaM sequence of $n+1$ through 148. $Sc^{1-129}/Gg^{130-148}$ binds only 3 mol of Ca^{2+} like recombinant yeast CaM and has low affinities for both PDE and MLCK (compare the K_{act} values in Table 1). These results indicate that $Sc^{1-129}/Gg^{130-148}$ has a low-affinity structure like yeast CaM, $Sc^{1-128}/Gg^{129-148}$ has a high-affinity structure for PDE but not skMLCK, and both Sc^{1-87}/Gg^{88-148} and Sc^{1-72}/Gg^{73-148} have a high-affinity structure (compare the V_{max} and K_{act} values in Table 1).

Further biochemical results have revealed that cooperative Ca^{2+} binding and a suitable rearrangement of a pair of Ca^{2+}-binding sites in each lobe are important for high-affinity interaction with PDE and that residues in chicken CaM sequences of $Gg^{129-148}$ and Gg^{88-128}, respectively, are required for low values of K_{act} in the activation of PDE and skMLCK (*16*). The difference in the structural requirements indicated different manners of interaction (*16*).

We do not as yet know the solution structure and interaction of these chimeric CaMs. Therefore, our interests have focused on the solution structure and the interaction of chimeric CaMs in an effort to reveal the molecular origin of the low-affinity and less active structure of yeast CaM. We used here small-angle X-ray scattering with synchrotron radiation (SR-SAXS) as a tool and a 22-residue peptide corresponding to the CaM-binding domain (residues 577−598) of skMLCK as a model peptide of the natural target for chimeric CaMs. The results presented here indicate that the replacement of Asp^{129} with Ser^{129} in site IV of CaM induces the intramolecular interaction between two lobes.

MATERIALS AND METHODS

Materials. Recombinant chimeric proteins of yeast and chicken CaM ($Sc^{1-129}/Gg^{130-148}$, $Sc^{1-128}/Gg^{129-148}$, Sc^{1-87}/Gg^{88-148}, and Sc^{1-72}/Gg^{73-148}) were produced by exactly the same procedure of protein engineering as previously described in detail (*16*). The concentration of proteins was determined by the method of Lowry et al. (*17*).

A 22-residue peptide having the sequence KRRWKKNFIAVSAANRFKKISS corresponding to the CaM-binding domain (residues 577−598) of skMLCK (termed MLCK-22p) was synthesized on an Applied Biosystem model 431 A peptide synthesizer using the general procedure. The crude MLCK-22p dissolved in water was filtered (Millipore filter, 0.45 μm) and purified with Sephadex G25 (Medium) (Pharmacia LKB) column (1.5 cm × 30 cm) chromatography. The purified MLCK-22p was freeze-dried and kept at −80 °C after weighing. The peptide was dissolved in water and used after the pH of the solution had been adjusted.

SR-SAXS Measurements. The measurements were performed using synchrotron orbital radiation with an instrument for SAXS installed at beamline BL-10C of the Photon Factory (Tsukuba, Japan). The details of the optics and instruments are given elsewhere (*18*). The basic medium used for the SAXS measurements consisted of 50 mM Tris-HCl (pH 7.6) and 120 mM NaCl; the molar ratios of Ca^{2+} denoted in this paper were added molar ratios of Ca^{2+} per mole of protein, and Ca^{2+}-free proteins were placed in 1 mM EDTA. The temperature of the SAXS experiment was kept at 25.0 °C by circulating water through the cell holder. The volume of the measuring cell was ca. 70 μL. The details of the sample preparation are given elsewhere (*11*).

Scattering Data Analysis. Two methods of data analysis were used. The first method is that of Guinier (*19*). The scattering intensity $I(s,c)$ measured as a function of s at a finite protein concentration, c, is given by

$$I(s,c) = I(0,c)\exp[-(4\pi^2/3)R_g(c)^2s^2] \quad (1)$$

where $I(0,c)$ is the scattering intensity at $s = 0$ and $R_g(c)$ is the radius of gyration at a concentration c, and s equals $(2\sin\theta)/\lambda$, where 2θ is the scattering angle and λ is the X-ray wavelength. In the dilute limit, $I(0,c)$ is given by

$$Kc/I(0,c) = 1/M + 2A_2c + ... \quad (2)$$

where K is a constant, M is the molecular weight of the protein, and A_2 is the second virial coefficient. In the dilute limit, $R_g(c)$ is given by

$$R_g(c)^2 = R_0^2 - B_{if}c + ... \quad (3)$$

where R_0 is the radius of gyration at infinite dilution and B_{if} is the parameter of interparticle interference (*20, 21*). According to Fournet, B_{if} is represented in terms of the interparticle force potential and the temperature, and the sign is usually the same as that of A_2 (*19*). Using eqs 2 and 3, we estimated the three parameters A_2, R_0, and B_{if}. For the analysis, the range of s^2 (Å^{-2}) was from 1.6×10^{-5} to 1.6×10^{-4} for all samples measured.

The second method is the calculation of the distance distribution function, $P(r)$. $P(r)$ is given by

$$P(r) = 8\pi\int I(s)\,(sr)\sin(2\pi sr)\,ds \quad (4)$$

Other details of the method of data analysis were described elsewhere (*22, 23*).

RESULTS

The Guinier plots [$\ln I(s,c)$ vs s^2] for $Sc^{1-128}/Gg^{129-148}$ and $Sc^{1-129}/Gg^{130-148}$ over the concentration series are shown in Figures 1 and 2, respectively. Panels A−C represent the scattering curves in the absence of both Ca^{2+} and MLCK-22p, in the presence of Ca^{2+}, and in the presence of both Ca^{2+} and MLCK-22p, respectively. In all of the samples

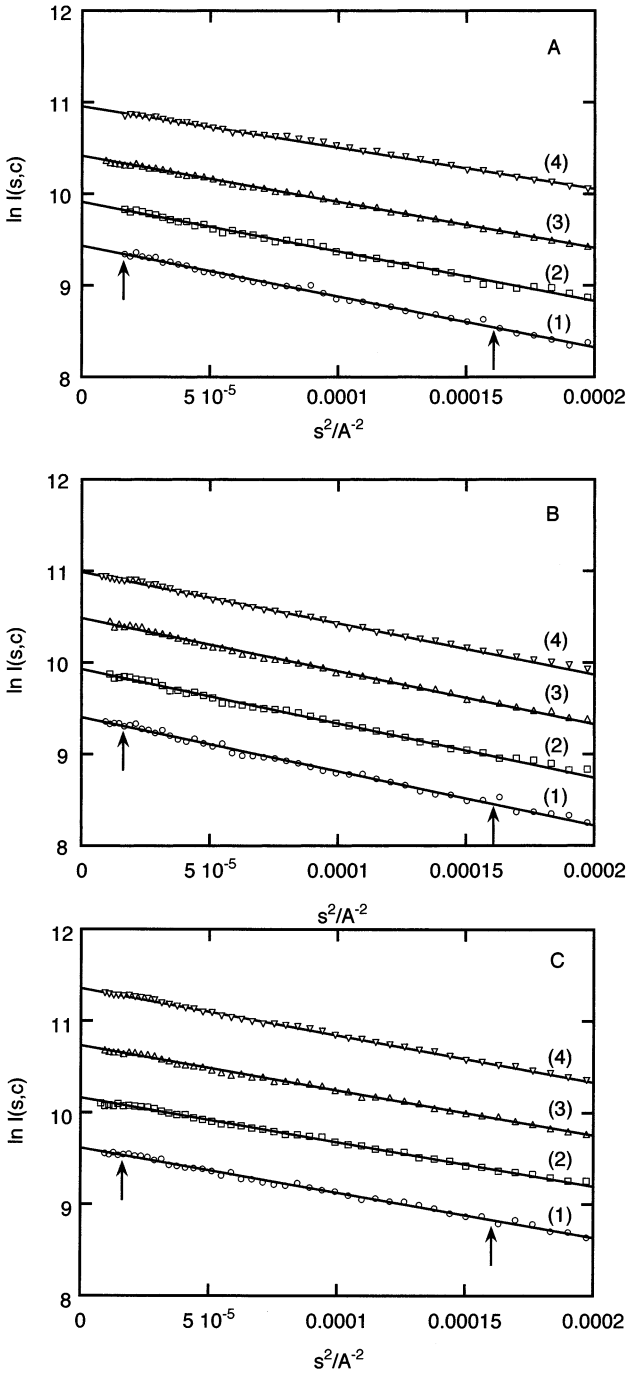

FIGURE 1: Guinier plots for the observed small-angle scattering from $Sc^{1-128}/Gg^{129-148}$ at a series of protein concentrations at pH 7.6. Panels A−C represent the scattering curves in the absence of both Ca^{2+} and MLCK-22p, in the presence of Ca^{2+}, and in the presence of both Ca^{2+} and MLCK-22p, respectively: (1) 7.5, (2) 10.0, (3) 15.0, and (4) 20.0 mg/mL. The straight lines were obtained with data points between the arrows in the figure by the least-squares method.

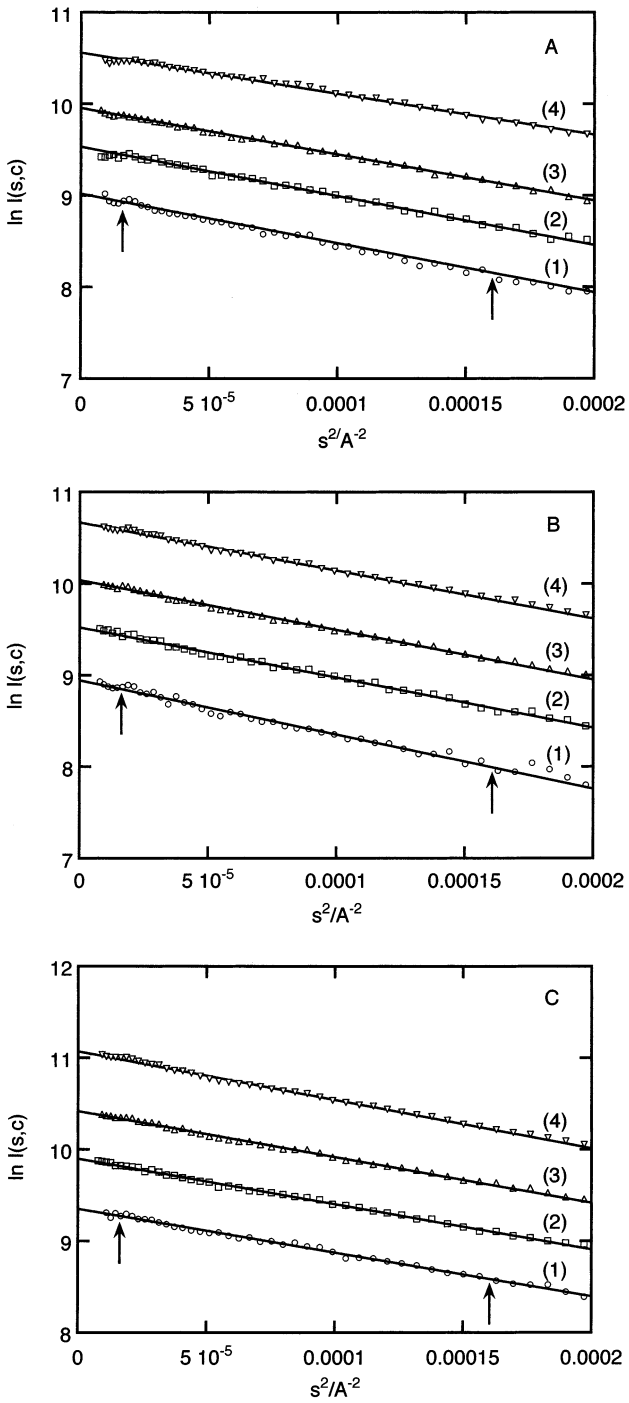

FIGURE 2: Guinier plots of SAXS from $Sc^{1-129}/Gg^{130-148}$ at a series of protein concentrations. The explanation is the same as in the legend of Figure 1.

studied here, including Sc^{1-72}/Gg^{73-148} and Sc^{1-87}/Gg^{88-148}, there is no evidence of any upward curvature at low s^2 values in the Guinier plots caused by aggregation of the samples, irrespective of the protein concentration (the Guinier plots for Sc^{1-72}/Gg^{73-148} and Sc^{1-87}/Gg^{88-148} are not shown). The values of $c/I(0,c)$ obtained from the intercepts of the Guinier plots are shown as a function of protein concentration in Figure 3, in which panels A and B depict data for $Sc^{1-128}/Gg^{129-148}$ and $Sc^{1-129}/Gg^{130-148}$, respectively. Plots in Figure 3 are also linear over the entire concentration range, and the values of $I(0,0)$ extrapolated to infinite dilution for these chimeric proteins under different conditions are proportional to the molecular weight appropriate for the soluble monomer. In these measurements, the absolute intensity of SR-SAXS from chimeras has not been compared quantitatively with the intensity scattered by a standard sample, because all samples have not been measured at the same period. The value of K was then determined by using the molecular weight calculated from the primary sequence of each chimera. The values of the second virial coefficient A_2 were calculated using eq 2 and compiled in Table 2. The negative values of A_2 for Ca^{2+}-saturated $Sc^{1-129}/Gg^{130-148}$ in the absence or the presence of MLCK-22p and for Ca^{2+}-saturated

Table 2: Second Virial Coefficient (A_2), Radius of Gyration Dilution (R_0), B_{if} Coefficient, and Center-to-Center Distance between Two Lobes (L) for CaMs under Three Different Conditions at pH 7.6[a]

	A_2 ($\times 10^4$ mol cm^3 g^{-2})			R_0 (Å)			B_{if} ($\times 10^{13}$ cm^5/g^2)			L (Å)		
	1	2	3	1	2	3	1	2	3	1	2	3
Bt^{1-148}	3.1	2.1	0.6	21.2	21.5	17.9	6.8	4.7	2.6	33.2	33.5	23.5
Sc^{1-72}/Gg^{73-148}	3.3	1.2	0.1	22.3	22.0	18.5	7.5	2.7	0.0	35.9	34.7	25.3
Sc^{1-87}/Gg^{88-148}	3.4	1.2	0.9	22.0	22.0	18.7	5.7	2.0	0.6	35.2	34.7	25.9
$Sc^{1-128}/Gg^{129-148}$	4.6	2.8	−0.7	21.6	21.9	18.9	6.2	2.5	−1.2	34.2	34.5	25.9
$Sc^{1-129}/Gg^{130-148}$	3.8	−0.3	−0.4	21.7	20.9	18.6	5.6	1.7	−2.4	34.4	31.9	25.6
Sc^{1-146}	7.1	0.1	2.5	21.1	19.9	18.3	4.7	−0.9	−0.1	32.9	29.2	24.7

[a] The definitions of A_2, R_0, B_{if}, and L are given in the text (eqs 2, 3, and 5). The values of A_2, R_0, B_{if}, and L of bovine CaM (*B. taurus*, Bt^{1-148}) and yeast CaM (Sc^{1-146}) are taken from a previous report (*24*). The numbers 1−3 represent the solution in the absence of Ca^{2+}, in the presence of Ca^{2+}, and in the presence of both Ca^{2+} and MLCK-22p, respectively.

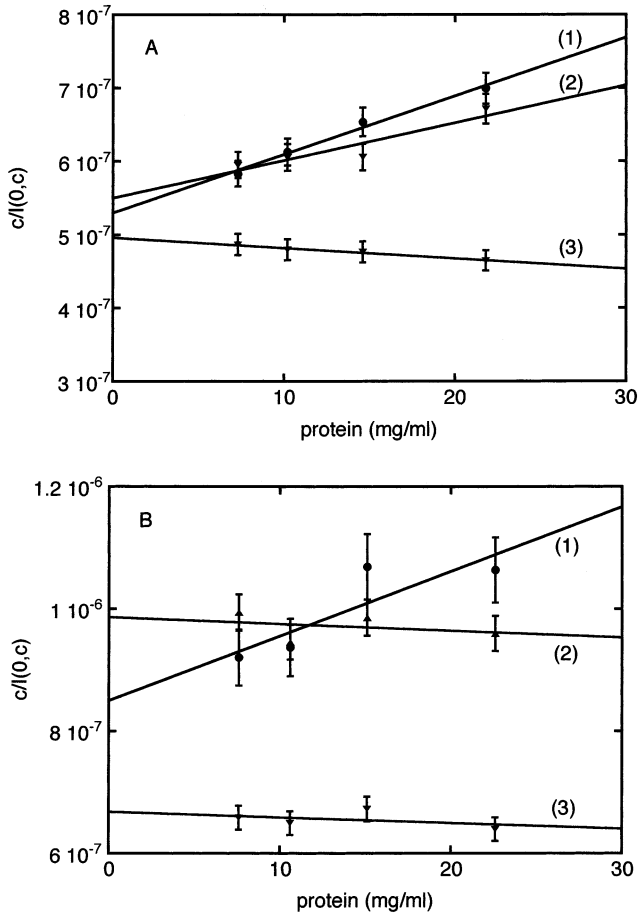

FIGURE 3: Protein concentration dependence of $c/I(0,c)$ measured at pH 7.6. The measured $c/I(0,c)$ as a function of protein concentration is plotted for $Sc^{1-128}/Gg^{129-148}$ (A) and $Sc^{1-129}/Gg^{130-148}$ (B) in the absence of both Ca^{2+} and MLCK-22p (1), in the presence of Ca^{2+} (2), and in the presence of both Ca^{2+} and MLCK-22p (3).

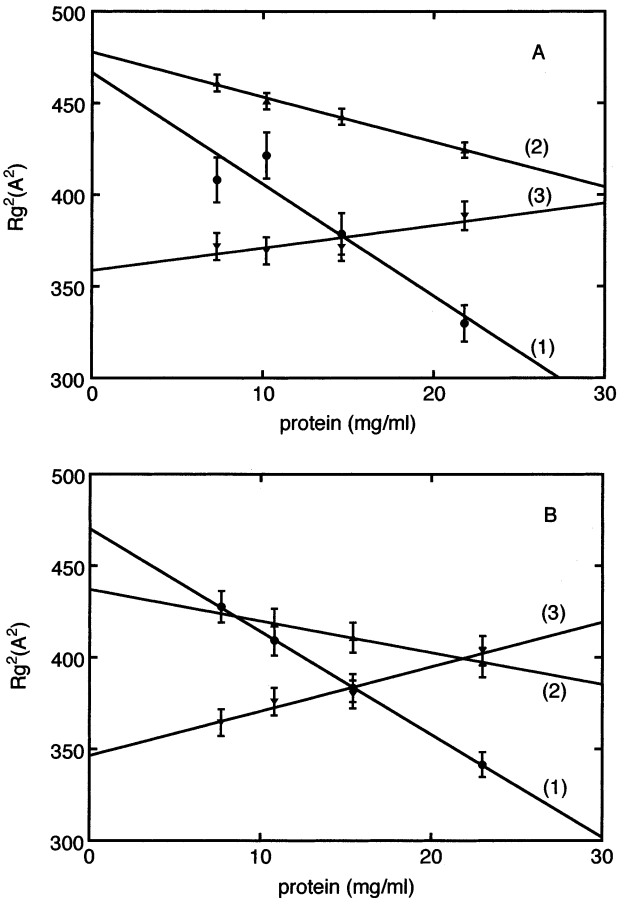

FIGURE 4: Protein concentration dependence of the measured radius of gyration at pH 7.6. The measured radius of gyration as a function of protein concentration is plotted for $Sc^{1-128}/Gg^{129-148}$ (A) and $Sc^{1-129}/Gg^{130-148}$ (B) in the absence of both Ca^{2+} and MLCK-22p (1), in the presence of Ca^{2+} (2), and in the presence of both Ca^{2+} and MLCK-22p (3).

$Sc^{1-128}/Gg^{129-148}$ in the presence of MLCK-22p indicate that the interactions between these chimeric proteins are attractive.

Apparent radii of gyration, $R_g(c)$, were calculated from the slopes of the Guinier plots using eq 1 and are shown as a function of protein concentration in Figure 4. The radii of gyration at infinite dilution, R_0, and the parameters of interparticle interference, B_{if}, were calculated using eq 3 and were compiled in Table 2. Table 2 also lists R_0, B_{if}, and A_2 values for Sc^{1-72}/Gg^{73-148} and Sc^{1-87}/Gg^{88-148}. The values of bovine (*Bos taurus*, Bt) CaM and yeast CaM were taken from our previous works (*24*). The negative values of B_{if} for $Sc^{1-129}/Gg^{130-148}$ and $Sc^{1-128}/Gg^{129-148}$ in the presence of both Ca^{2+} and MLCK-22p indicate that the interaction between the chimeric proteins is attractive. It is noted that the value of B_{if} for $Sc^{1-129}/Gg^{130-148}$ in the presence of Ca^{2+} is positive, while the corresponding value of A_2 is negative, suggesting that their interactions are remarkably specific.

In the absence of Ca^{2+}, the R_0 values for the chimeric CaMs are larger than those of bovine CaM and yeast CaM, although the molecular states resemble that of bovine CaM. Once Ca^{2+} binds, however, only the R_0 value of $Sc^{1-129}/Gg^{130-148}$ decreases ~4%, although the decrement is slightly small compared with that of yeast CaM (the decrement is ~6%), indicating that the replacement of Asp^{129} with Ser^{129} is necessary to bring the two lobes of CaM close together

and to form a novel compact structure of yeast CaM suggested recently (*11*, *12*, *14*). The SAXS results suggest that the interaction between $Sc^{1-129}/Gg^{130-148}$ CaMs is characterized by both a negative A_2 and a positive B_{if}, and it induces a novel compact structure.

In the presence of both Ca^{2+} and MLCK-22p, the R_0 values of all chimeric CaMs decreased, indicating that conformational changes toward a contracted form were induced by the binding of the peptide. The R_0 value of $Sc^{1-129}/Gg^{130-148}$ shows no significant difference compared with those of other chimeric CaMs, suggesting that the solution structures of these chimeric CaMs take a similar compact globular form. However, their interactions show a significant difference: $Sc^{1-128}/Gg^{129-148}$ and $Sc^{1-129}/Gg^{130-148}$ are characterized by negative values of A_2 and B_{if}.

In the absence of Ca^{2+}, all $P(r)$ profiles of chimeric CaMs have a maximum around 20 Å and a clear hump around 40 Å (Figure 5A). The solution structure of these chimeric CaMs is a dumbbell-like shape in which the two lobes, with a diameter of ~20 Å, are connected at a distance of ~40 Å. The R_0 values of these chimeric CaMs are consistent with this conclusion.

Under the Ca^{2+}-saturated condition, the $P(r)$ profiles of Sc^{1-72}/Gg^{73-148}, Sc^{1-87}/Gg^{88-148}, and $Sc^{1-128}/Gg^{129-148}$ have a maximum around 20 Å and a clear hump around 40 Å (Figure 5B). The solution structure of these chimeric CaMs is a dumbbell-like shape similar to that of Ca^{2+}-saturated bovine CaM. On the other hand, the $P(r)$ profile of $Sc^{1-129}/Gg^{130-148}$ has a maximum around 22 Å but an unclear hump around 40 Å. This is quite different from the findings for bovine CaM and other chimeric CaMs, suggesting that the solution structure of $Sc^{1-129}/Gg^{130-148}$ less resembles a dumbbell and takes an intermediate structure between bovine CaM and yeast CaM. The comparison between the solution structures of $Sc^{1-128}/Gg^{129-148}$ and $Sc^{1-129}/Gg^{130-148}$ provides direct evidence that the replacement of Asp^{129} with Ser^{129} induces an interaction between two lobes of CaM and brings them close together. It implies that the site IV that is unable to bind Ca^{2+} hinders the ability of the C-lobe to undergo the conformational change to the full open state and a site interacting with the N-lobe is induced in the C-lobe.

In the presence of both Ca^{2+} and MLCK-22p, all $P(r)$ profiles of chimeric CaMs display a single peak around 23 Å without any hump. The chimeric CaMs have a less compact globular shape than the complex of Ca^{2+}-saturated vertebrate CaM with the target peptide (*11*, *25*, *26*), which is consistent with the results from the R_0 values. The results suggest that the C-lobe of these chimeric CaMs also behaves as a globular domain in the formation of the complex.

DISCUSSION

In the development of a molecular explanation for the SR-SAXS data, it is useful that the structure of chimeric CaMs consists of two quite separate but globular domains with an interconnecting helix. The radius of gyration at infinite dilution, R_0, may be given by

$$R_0^2 = R_{lobe}^2 + L^2/4 \quad (5)$$

where R_{lobe} is the radius of gyration of a lobe and L is the center-to-center distance between two lobes (*27*). From eq 5, the value of L is calculated using an R_{lobe} of 13.2 Å in the absence of Ca^{2+} and an R_{lobe} of 13.5 Å in the presence of Ca^{2+} (*22*). The results are compiled in Table 2. Here the assumption of a fixed R_{lobe} seems to be inconsistent with the fact that both yeast CaM and $Sc^{1-129}/Gg^{130-148}$ do not bind Ca^{2+} in site IV, which might suggest an altered tertiary structure. However, it is shown that a small change in R_{lobe} does not almost change the L values. Furthermore, as described in the Results and later, a site interacting with the N-lobe is induced in the C-lobe of $Sc^{1-129}/Gg^{130-148}$ under the Ca^{2+}-saturated condition, suggesting that the C-lobe behaves as a globular domain, and the C-lobe of all chimeric CaMs behaves as a globular domain in the formation of the complex. It is noted that the values of L for chimeric CaMs

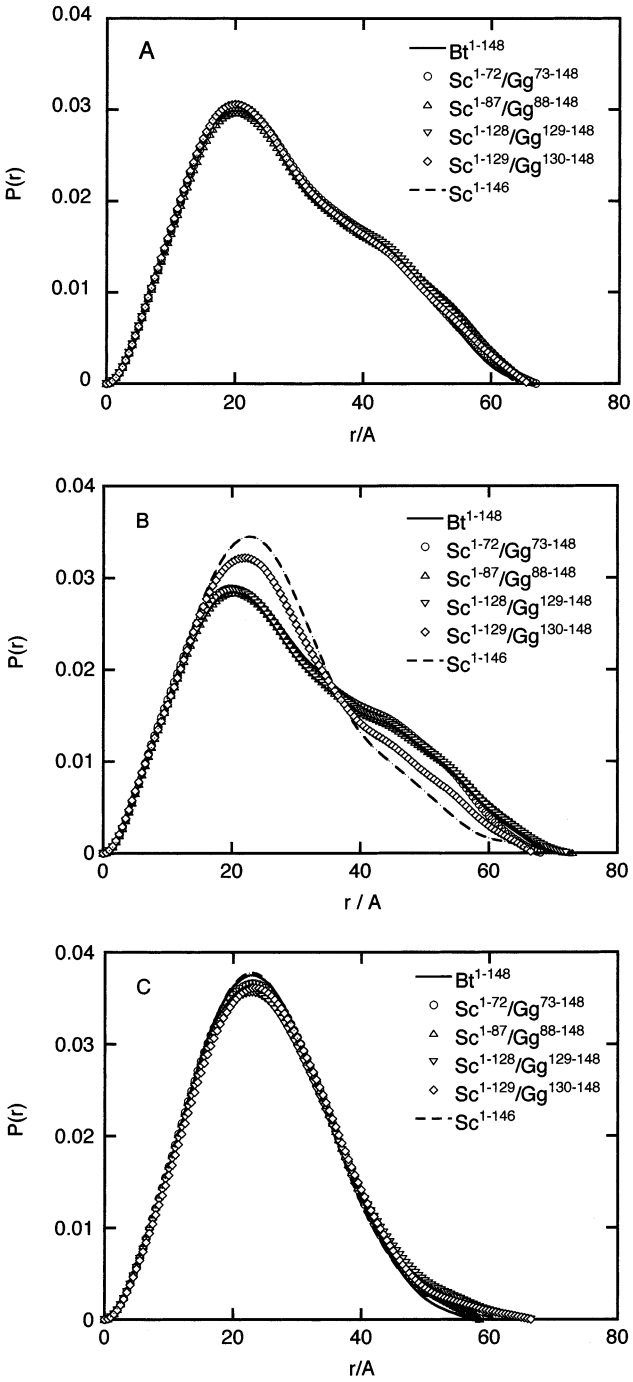

FIGURE 5: Distance distribution function, $P(r)$, of various CaMs at pH 7.6. Panels A−C represent the $P(r)$ profiles of the CaMs in the absence of both Ca^{2+} and MLCK-22p, in the presence of Ca^{2+}, and in the presence of both Ca^{2+} and MLCK-22p.

in the absence of Ca^{2+} are always larger than that for bovine CaM, suggesting that the solution structure of chimeric CaMs is a slightly extended dumbbell-like structure compared to that of bovine CaM. The Ca^{2+} binding to Sc^{1-72}/Gg^{73-148}, Sc^{1-87}/Gg^{88-148}, and $Sc^{1-128}/Gg^{129-148}$ causes an increase in the value of L compared with that of bovine CaM. However, it induces a decrease in $Sc^{1-129}/Gg^{130-148}$, indicating the direct evidence of an attractive interaction between two lobes, which originates from the replacement of Asp^{129} with Ser^{129}. In the presence of both Ca^{2+} and the target peptide, the values of L for the complexes of chimeric CaMs are always larger than that of bovine CaM, suggesting that the solution structures in the complex of chimeric CaMs have a slightly relaxed globular structure compared to that of bovine CaM.

Comparisons between Bovine CaM and Sc^{1-72}/Gg^{73-148}. The $P(r)$ profiles of Sc^{1-72}/Gg^{73-148} and bovine CaM exhibit similar behaviors as shown in Figure 5, suggesting that the solution structure of Sc^{1-72}/Gg^{73-148} is similar to that of bovine CaM. However, the structural and interaction parameters for Sc^{1-72}/Gg^{73-148} are apparently different from those of bovine CaM. These differences result from the replacement of amino acid residues Met^{51}, Met^{71}, Lys^{30}, and Val^{55} in bovine CaM with Leu^{51}, Leu^{71}, Ser^{30}, and Ile^{55}, respectively, in Sc^{1-72}/Gg^{73-148}. Particularly, in the presence of Ca^{2+}, the hydrophobic surface in the N-lobe of Sc^{1-72}/Gg^{73-148} loses its flexibility, resulting in the hydrophobic surface being smaller than in the case of bovine CaM (*15*, *28*). The result suggests that a repulsive interaction is more dominant in Sc^{1-72}/Gg^{73-148} than in bovine CaM. Consequently, the structural parameters such as R_0 and L of Sc^{1-72}/Gg^{73-148} are larger than those of bovine CaM, while the interaction parameters such as B_{if} and A_2 are smaller than those of bovine CaM.

Comparisons between Sc^{1-72}/Gg^{73-148} and Sc^{1-87}/Gg^{88-148}. The replacements of Ala^{73}, Lys^{75}, Met^{76}, Asp^{78}, Glu^{83}, and Arg^{86} in Sc^{1-72}/Gg^{73-148} with Ser^{73}, Gln^{75}, Leu^{76}, Ser^{78}, Gln^{83}, and Leu^{86}, respectively, in Sc^{1-87}/Gg^{88-148} do not show a significant difference, suggesting that the central linker is less sensitive to these replacements.

Comparisons between Sc^{1-87}/Gg^{88-148} and $Sc^{1-128}/Gg^{129-148}$. The SAXS results of Sc^{1-87}/Gg^{88-148} and $Sc^{1-128}/Gg^{129-148}$ do not show a significant difference except those in the presence of both Ca^{2+} and the target peptide. It is suggested that Met^{109} and Glu^{119} play a critical role in the target recognition, as the sign in the B_{if} and A_2 values of Sc^{1-87}/Gg^{88-148} and $Sc^{1-128}/Gg^{129-148}$ is inverted under this condition, as shown in Table 2. The role of Glu^{119} has not been reported hitherto. The difference in these interaction parameters could explain the differences in V_{max} and K_{act} of Sc^{1-87}/Gg^{88-148} and $Sc^{1-128}/Gg^{129-148}$.

Comparisons between $Sc^{1-128}/Gg^{129-148}$ and $Sc^{1-129}/Gg^{130-148}$. Under the Ca^{2+}-saturated condition, the solution structure of $Sc^{1-129}/Gg^{130-148}$ is substantially different from that of $Sc^{1-128}/Gg^{129-148}$. On the basis of the structural parameters, particularly the values of R_0 and the $P(r)$ profiles, it is reasonable to consider an intermediate structure between bovine CaM and yeast CaM for $Sc^{1-129}/Gg^{130-148}$. $Sc^{1-128}/Gg^{129-148}$ binds Ca^{2+} at sites I−IV, while $Sc^{1-129}/Gg^{130-148}$ bind Ca^{2+} at three of the sites (not site IV). In $Sc^{1-128}/Gg^{129-148}$, the binding of Ca^{2+} induces a concerted opening to each lobe and a drastic change in the helix packing of each lobe. The solution structure of $Sc^{1-128}/Gg^{129-148}$ is a dumbbell-like structure similar to that of bovine CaM. In $Sc^{1-129}/Gg^{130-148}$, however, the concerted opening does not occur in the C-lobe but in the N-lobe; that is, the drastic change in the helix packing does not occur in the C-lobe but in the N-lobe. Although the change in the interhelical distance of the F−G helix pair in Ca^{2+}-saturated vertebrate CaM is similar to that of Ca^{2+}-free vertebrate CaM, the corresponding interhelical angle is quite different from another (*29*−*31*). Although it is suggested that the C-lobe of $Sc^{1-129}/Gg^{130-148}$ adopts an unusual helix packing which is not seen in $Sc^{1-128}/Gg^{129-148}$, we could regard the C-lobe as a novel globular domain different from that of $Sc^{1-128}/Gg^{129-148}$. The novel solution structure of $Sc^{1-129}/Gg^{130-148}$ could be modeled as a composite of sites I−III of Ca^{2+}-saturated vertebrate CaM and site IV of Ca^{2+}-free vertebrate CaM, in which sites I−IV are formed by A−B, C−D, E−F, and G−H helices, respectively (*29*). Consequently, the solvent-exposed hydrophobic surface of the C-lobe in $Sc^{1-129}/Gg^{130-148}$, which is partially surrounded by acidic residues, is quite different from that of $Sc^{1-128}/Gg^{129-148}$, although that of the N-lobe is the same as that of $Sc^{1-128}/Gg^{129-148}$. These unbalances between the N- and C-lobes of $Sc^{1-129}/Gg^{130-148}$ affect both the solution structure and their interactions, and bring the two lobes close together. The SAXS results are consistent with these interpretations. It should be noted, however, that the Ca^{2+} -free form of $Sc^{1-129}/Gg^{130-148}$ has a dumbbell-like structure similar to that of $Sc^{1-129}/Gg^{130-148}$.

In the presence of both Ca^{2+} and MLCK-22p, the solution structure of $Sc^{1-129}/Gg^{130-148}$ is a globular structure similar to that of $Sc^{1-128}/Gg^{129-148}$. On the basis of the interaction parameters, particularly values of B_{if} and A_2, however, the interaction of $Sc^{1-129}/Gg^{130-148}$ is quite different from that of $Sc^{1-128}/Gg^{129-148}$. The results suggest that the globular structure of $Sc^{1-129}/Gg^{130-148}$ complexed with the target peptide is apparently stabilized by the electrostatic and van der Waals interactions different from those of $Sc^{1-128}/Gg^{129-148}$.

Comparisons between $Sc^{1-129}/Gg^{130-148}$ and Yeast CaM. In the absence of Ca^{2+}, the $P(r)$ profiles of $Sc^{1-129}/Gg^{130-148}$ and yeast CaM exhibit a similar behavior as shown in Figure 5A, suggesting that these solution structures are a dumbbell-like structure similar to that of bovine CaM. On the basis of the values of R_0, it is reasonable for yeast CaM to consider a dumbbell-like structure more compact than that of $Sc^{1-129}/Gg^{130-148}$.

Yeast CaM like $Sc^{1-129}/Gg^{130-148}$ binds Ca^{2+} to other three sites except site IV. On the basis of the structural parameters, particularly the values of R_0 and $P(r)$ profiles, the Ca^{2+} binding to yeast CaM induces a structure more compact than that of $Sc^{1-129}/Gg^{130-148}$. The solution structure of yeast CaM is an intermediate structure between a dumbbell-like structure and a compact globular structure. The difference in the solution structure between yeast CaM and $Sc^{1-129}/Gg^{130-148}$ is responsible for the helix packing in their C-lobe, which originates from differences between residues in chicken CaM residues 130−148 and those in yeast CaM residues 130−146.

In the presence of both Ca^{2+} and MLCK-22p, the solution structure of yeast CaM is a compact globular structure similar to that of $Sc^{1-129}/Gg^{130-148}$. On the basis of the interaction parameters, particularly values of B_{if} and A_2, however, the interaction of yeast CaM is substantially different from that

of $Sc^{1-129}/Gg^{130-148}$. The results suggest that the globular structure of yeast CaM complexed with the target peptide is apparently stabilized by the electrostatic and van der Waals interactions different from those of $Sc^{1-129}/Gg^{130-148}$.

The results presented here indicate that the replacement of residue 119 in site IV of CaM changed the interactions between CaMs, while that of residue 129 induced the intramolecular interaction between two lobes. Furthermore, these SAXS results are consistent with previous V_{max} and K_{act} determinations with skMLCK and with PDE (*16*). If one could compare the scattering from $Sc^{1-128}/Gg^{129-148}$ with that of $Gg^{1-128}/Sc^{129-148}$, one would predict the following. These two would have a similar dumbbell-like structure in the absence of Ca^{2+} and a similar compact globular shape in the presence of both Ca^{2+} and MLCK-22p, while these two would have a different structure under the Ca^{2+}-saturated condition; i.e., $Sc^{1-128}/Gg^{129-148}$ takes a dumbbell-like structure, while $Gg^{1-128}/Sc^{129-148}$ has an intermediate structure between the dumbbell-like shape and the compact globular shape. The intermediate structure should originate from the differences in the residues of $Sc^{129-148}$ containing Ser^{129}.

To study the interaction of CaM with the intact skMLCK, we used MLCK-22p as the model peptide in this report. This may only imperfectly mimic the interaction of CaM with the intact skMLCK. Further studies will be needed to confirm this point.

ACKNOWLEDGMENT

We thank Dr. Katsumi Kobayashi for help in the SR-SAXS measurements.

REFERENCES

1. Babu, Y. S., Bugg, C. E., and Cook, W. J. (1988) *J. Mol. Biol. 204*, 191−204.
2. Kretsinger, R. H., Rudnick, S. E., and Weissman, L. J. (1986) *J. Inorg. Biochem. 28*, 289−302.
3. Chattopadhyaya, R., Meador, W. E., Means, A. R., and Quiocho, F. A. (1992) *J. Mol. Biol. 228*, 1177−1192.
4. Yazawa, M., Ikura, M., Hikichi, K., Ying, L., and Yagi, K. (1987) *J. Biol. Chem. 262*, 10951−10954.
5. Toda, H., Yazawa, M., Sakiyama, F., and Yagi, K. (1985) *J. Biochem. 98*, 833−842.
6. Ohya, Y., Uno, I., Ishikawa, T., and Anraku, Y. (1987) *Eur. J. Biochem. 168*, 13−19.
7. Luan, Y., Matsuura, I., Yazawa, M., Nakamura, T., and Yagi, K. (1987) *J. Biochem. 102*, 1531−1537.
8. Starovasnik, A. M., Davis, T. N., and Klevit, R. E. (1993) *Biochemistry 32*, 3261−3270.
9. Davis, T. N., Urdea, M. S., Masiarz, R. F., and Thorner, J. (1986) *Cell 47*, 423−431.
10. Matsuura, I., Ishihara, K., Nakai, Y., Yazawa, M., and Yagi, K. (1991) *J. Biochem. 109*, 190−197.
11. Yoshino, H., Izumi, Y., Sakai, K., Takezawa, H., Matsuura, I., Maekawa, H., and Yazawa, M. (1996) *Biochemistry 35*, 2388−2393.
12. Nakashima, K., Ishida, H., Ohki, S., Hikichi, K., and Yazawa, M. (1999) *Biochemistry 38*, 98−104.
13. Yazawa, M., Nakashima, K., and Yagi, K. (1999) *Mol. Cell. Biochem. 190*, 47−54.
14. Lee, S. Y., and Klevit, R. E. (2000) *Biochemistry 39*, 4225−4230.
15. Ishida, H., Takahashi, K., Nakashima, K., Kumaki, Y., Nakata, M., Hikichi, K., and Yazawa, M. (2000) *Biochemistry 39*, 13660−13668.
16. Nakashima, K., Maekawa, H., and Yazawa, M. (1996) *Biochemistry 35*, 5602−5010.
17. Lowry, O. H., Rosebrough, N. J., Farr, A. L., and Randall, R. J. (1951) *J. Biol. Chem. 193*, 265−275.
18. Ueki, T., Hiragi, Y., Kataoka, M., Inoko, Y., Amemiya, Y., Izumi, Y., Tagawa, H., and Muroga, Y. (1985) *Biophys. Chem. 23*, 115−124.
19. Guinier, A., and Fournet, G. (1955) *Small-Angle Scattering of X-ray*, pp 24−28, 40−52, 57−60, 135−136, Wiley, New York.
20. Izumi, Y., Wakita, M., Yoshino, H., and Matsushima N. (1992) *Biochemistry 31*, 12266−12271.
21. Izumi, Y., Kuwamoto, S., Jinbo, Y., and Yoshino, H. (2001) *FEBS Lett. 495*, 126−130.
22. Matsushima, N., Izumi, Y., Matsuo, T., Yoshino, H., Ueki, T., and Miyake, Y. (1989) *J. Biochem. 105*, 883−887.
23. Yoshino, H., Minari, O., Matsushima, N., Ueki, T., Miyake, Y., Matsuo, T., and Izumi, Y. (1989) *J. Biol. Chem. 264*, 19706−19709.
24. Izumi, Y., Nogami, H., Yokouchi, T., Yoshino, H., and Yazawa, M. (1996) *Photon Factory Activity Rep. 14*, 251.
25. Ikura, M., Marius Clore, G., Gronenborn, A. M., Zhu, G., Klee, C. B., and Bax, A. (1992) *Science 256*, 632−638.
26. Meador, W. E., Means, A. R., and Quiocho, F. A. (1992) *Science 257*, 1251−1255.
27. Anderegg, J. W., Beeman, W. W., Shulman, S., and Kaesberg, P. (1955) *J. Am. Chem. Soc. 77*, 2927−2937.
28. Zhang, M., Li, M., Wang, J. H., and Vogel, H. J. (1994) *J. Biol. Chem. 269*, 15546−15552.
29. Zhang, M., Tanaka, T., and Ikura, M. (1995) *Nat. Struct. Biol. 2*, 758−767.
30. Kuboniwa, H., Tjandra, N., Grzesiek, S., Ren, H., Klee, C. B., and Bax, A. (1995) *Nat. Struct. Biol. 2*, 768−776.
31. Finn, B. E., Evenas, J., Dralenberg, T., Waltho, J. P., Thulin, E., and Forsen, S. (1995) *Nat. Struct. Biol. 2*, 777−783.

BI020501S